nature research

https://doi.org/10.1038/s41563-020-0789-2

Supplementary information

A bioinspired and hierarchically structured shape-memory material

In the format provided by the authors and unedited

Supporting Information

A Bioinspired and Hierarchically Structured Shape Memory Material

By *Luca Cera, Grant M. Gonzalez, Qihan Liu, Suji Choi, Christophe O. Chantre, Juncheol Lee, Myung C. Choi, Rudy Gabardi, Kwanwoo Shin, and Kevin Kit Parker**

Table of contents

Supplementary Video 1. **Shape memory fibers.**

Images shown in Figures 3g are taken from this video.

The yarn was produced by manually twisting a fiber strand of same diameter size (~ 30 microns), which are blocked together with knots at both edges. The yarn is immersed into deionized water for a few seconds, manually stretched while still in a wet state and kept under load at room temperature for about 10 minutes. When weights are removed to allow the yarn to relax, no visible change in length between the stretched and relaxed form is observed by the naked eye. To show the ability of the yarn to recover its original length nebulized water is applied. Indeed, shrinking of the fibers leads to reshaping of the yarn to its original length only in a few seconds.

Supplementary Video 2. **Shape memory 3D printed scaffolds.**

Images shown in Figures 4f are taken from this video.

The 3D printed star-shaped origami is locked in a rolled-tube temporary configuration and hydrated to regain its original permanent architecture. This happens after a few seconds of hydration, when the keratin rolled tube starts an unfolding process caused by flattering of the bended surfaces. Closure of the final origami is achieved as the star edges are reformed and fold back in a cooperative fashion.

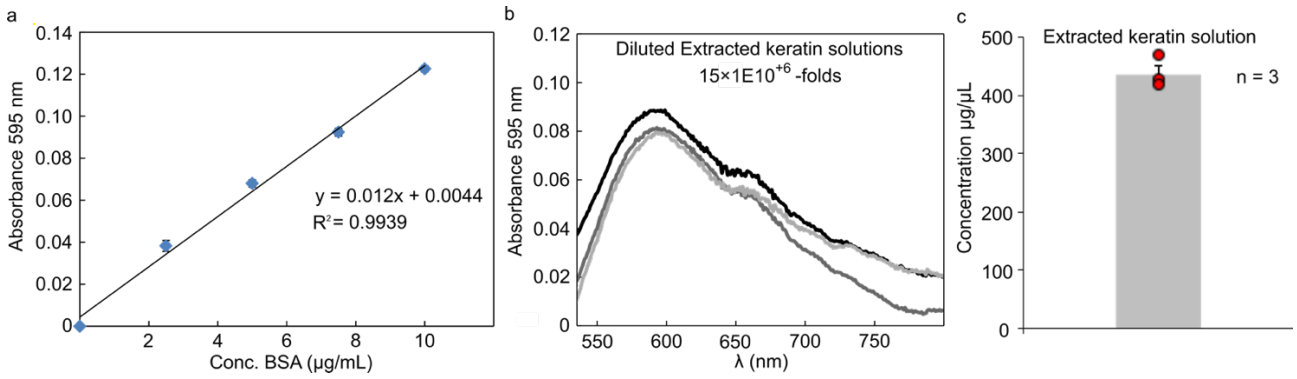

Supplementary Figure 1. Determination of keratin concentration by using the Bradford assay. a) Standard curve obtained from known bovine serum albumin (BSA) concentrations using the Bradford assay (n = 3 sample tested per each concentration of BSA). b) UV-Vis absorption spectra of $15\times1E10^{+6}$ diluted samples of extracted keratin (n = 3 independent keratin

extraction batches tested). c) Bar graph with associated scattering plot showing the protein concentration of the extracted keratin solution of 401.7 ± 15 mg/mL (n = 3 independent keratin extraction batches tested). Data are presented as mean values +/- SEM.

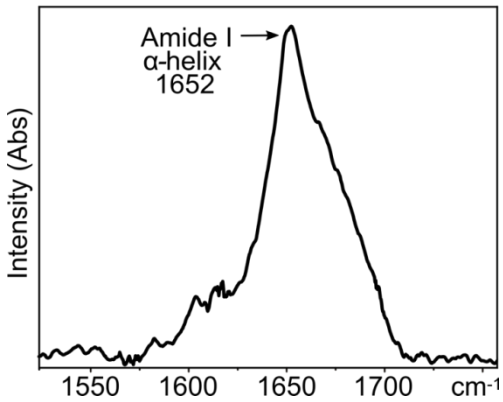

Supplementary Figure 2. Raman spectroscopy of a dry sample of the extracted keratin. The analysis was performed on a keratin sample purified via dialysis against water (1 L×3) over 48 hours and freeze-dried. The retainment of the α-helix secondary structure during extraction is supported by the presence of the characteristic band at 1652 cm^{-1}.[1]

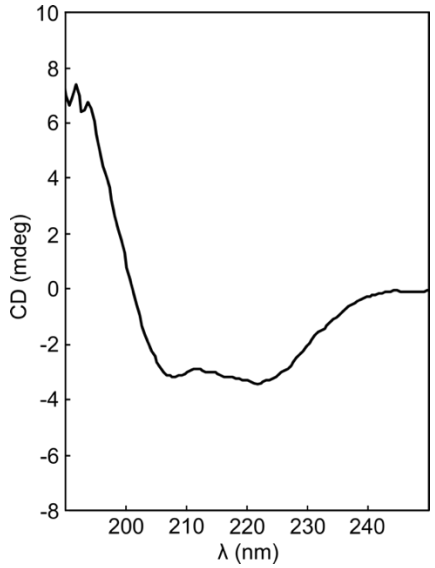

Supplementary Figure 3. α-helix coiled-coil structure characterization using circular dichroism CD. Spectrum of the extracted keratin solution in water at pH 5.6 (0.2 mg/mL) and using a cuvette with a 5 mm path-length. The presence of the positive band at 192 nm and the negative bands at 208 and 222 nm supports the α-helix conformation of keratin in solution.[2]

Furthermore, the intensity ratio between the band at 222 nm and the band at 208 nm (R2 = 222nm/208nm) is greater than 1, indicating the arrangement of the paired α-helices in the coiled-coil architecture.[3]

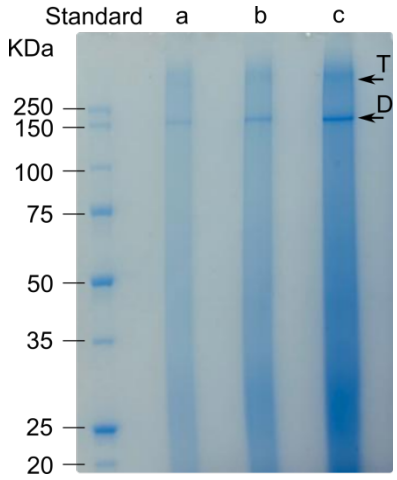

Supplementary Figure 4. SDS-Page of the extracted keratin solution. Concentration-dependent SDS-Page analysis carried out on the extracted keratin solution, using a 10% acrylamide gel and a Tris/Glycine/SDS running buffer. Samples were prepared by mixing 5 µL of a 50-folds diluted solution of the extracted keratin (diluted in a 3M LiBr water solution) with a) 80 µL, b) 40 µL and c) 20 µL of Laemmli buffer containing DTT (50 mM). After gel fixation using a water solution of isopropyl alcohol (25% v/v) and acetic acid (10% v/v), the gel was stained using a water solution of acetic acid (10 % v/v) and Coomassie blue 60 (mg/L). The presence of the main band at ~150 kDa belonging to α-helix dimer (D) and the one at higher molecular weights, belonging to the tetramer (T), supports the successful preservation of the coiled-coil structure during extraction and few degradation products.[4] Although no characteristic bands in the 40-60 KDa range are observed, Angora wool keratin is known to be a heterodimeric polymer.[5] The SDS-Page experiment was carried out 3 times for a Laemmli solution concentration of 40 µL.

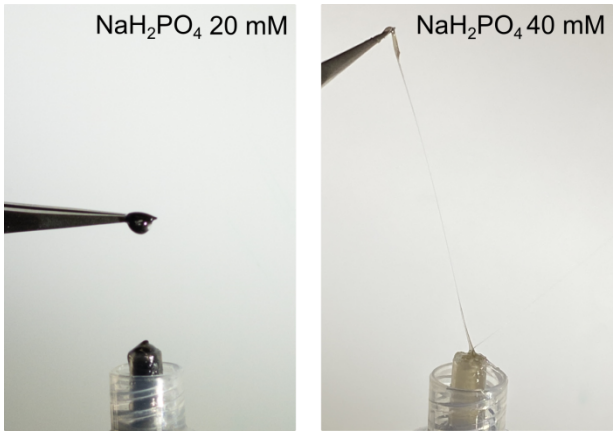

Supplementary Figure 5. Pulling fibers from keratin solution. Photographs of the extracted keratin solutions (401.7 mg/mL) containing 20 mM (left) and 40 mM (right) of NaH_2PO_4. At concentration of NaH_2PO_4 lower than 40 mM, the lower degree of keratin self-assembly hinders fiber formation when the solution is pulled with a tweezer.

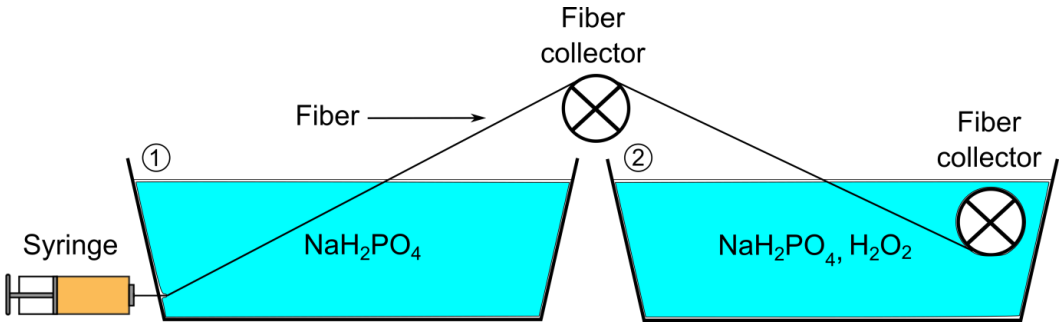

Supplementary Figure 6. Keratin fibers wet-spinning protocol and set-up. Schematic of the wet-spinning platform used to produce keratin fibers. The platform consists of a syringe pump and two coagulation baths placed in series with independent polytetrafluoroethylene (PTFE) collectors. At room temperature, the keratin dope is infused at a 10 µL/min of rate into the first coagulation bath containing a water solution of NaH_2PO_4, at a pH lower than the average keratin isoelectric point (0.4 M, pH 4.3).[6] A needle of 27 gauge is used (needle length 3 cm, McMaster-Car). Fibers are collected after the first coagulation bath and continuously drawn into the second coagulation bath containing a water solution of NaH_2PO_4 (0.8 M) and H_2O_2 (1%). The two reaction steps were located in different and sequential baths to allow for the complete coagulation of the protein before forming the disulfide covalent network, because the H_2O_2-assisted oxidation occurs with a fast kinetic.[7]

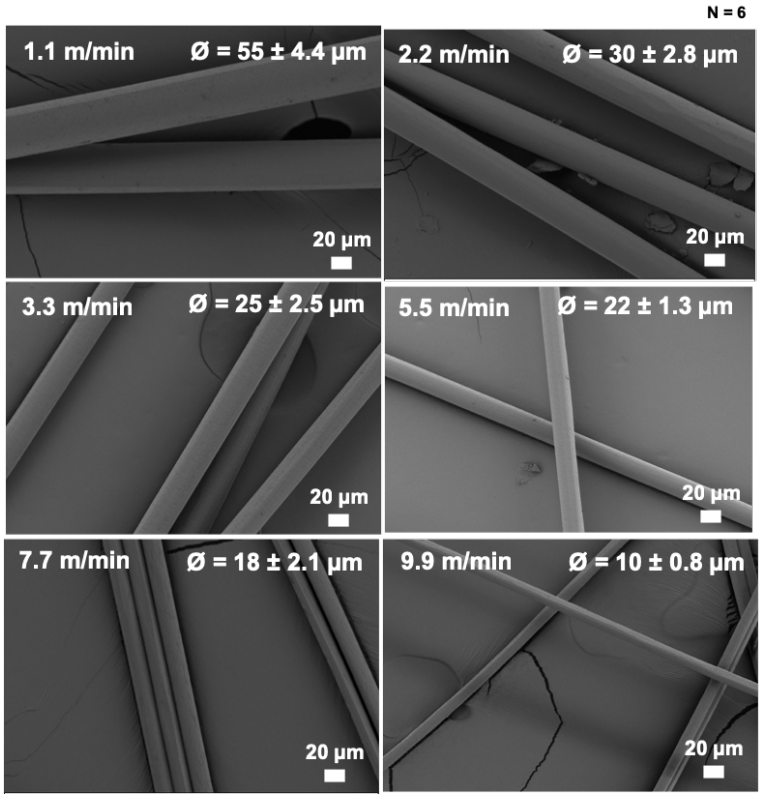

Supplementary Figure 7. Tuning of keratin fiber diameter. SEM micrographs of keratin fibers obtained at different collection speeds. As shown in the image, the fiber diameter can be finely tuned by increasing the speed of the second collector. Furthermore, the small standard error of the mean calculated for the average diameter size shows high accuracy and stability of the spinning process (n = 6 fibers tested per experimental condition; data are presented as mean values with experimental errors +/- calculated as SEM).

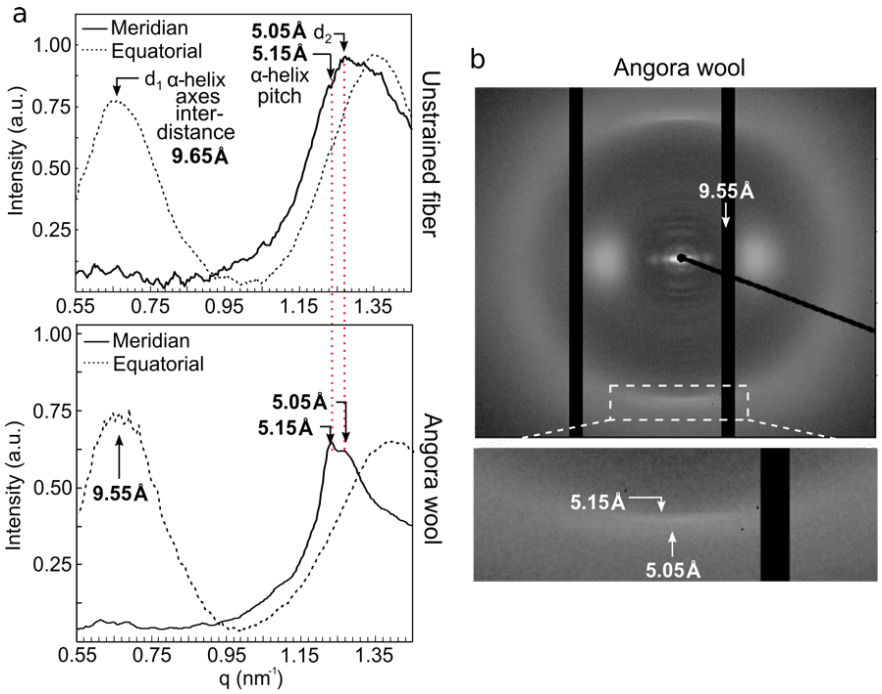

Supplementary Figure 8. 2D WAXS pattern comparison between the unstretched keratin fiber and wool. a) Comparison of the meridian and equatorial scattering profiles between the regenerated keratin fiber and Angora wool. The meridian shoulder at 5.15 Å and maximum at 5.05 Å of the regenerated fiber match with the meridian and off-meridian reflections of Angora wool (respectively), suggesting the presence of coiled-coils aligned along the fiber axis. Compared to the natural fiber however, the meridian reflections of the regenerated keratin fiber are broader, indicating the coiled-coils to be less crystalline and have a lower degree of alignment. b) 2D WAXS pattern of Angora wool showing the characteristic reflections at 9.55 Å belonging to the α-helix axes inter-distance, and the meridian and off-meridian reflections at 5.15 Å and 5.05 Å belonging to the α-helix pitch projection.[8,9]

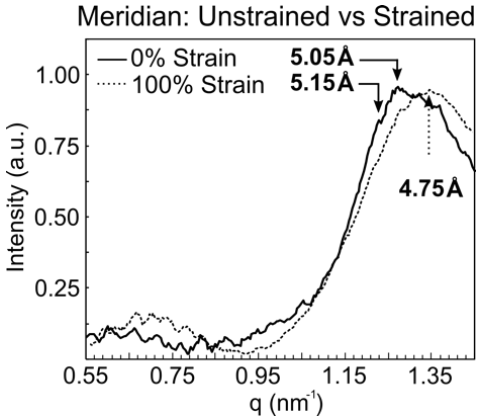

Supplementary Figure 9. WAXS Equatorial scattering profiles of unstrained and strained keratin fibers. Meridian scattering profiles of the unstrained and strained keratin fibers. The decrease in intensity of the 5.15 Å and 5.05 Å peaks supports the uncoiling of the alpha-helices upon fiber stretching.

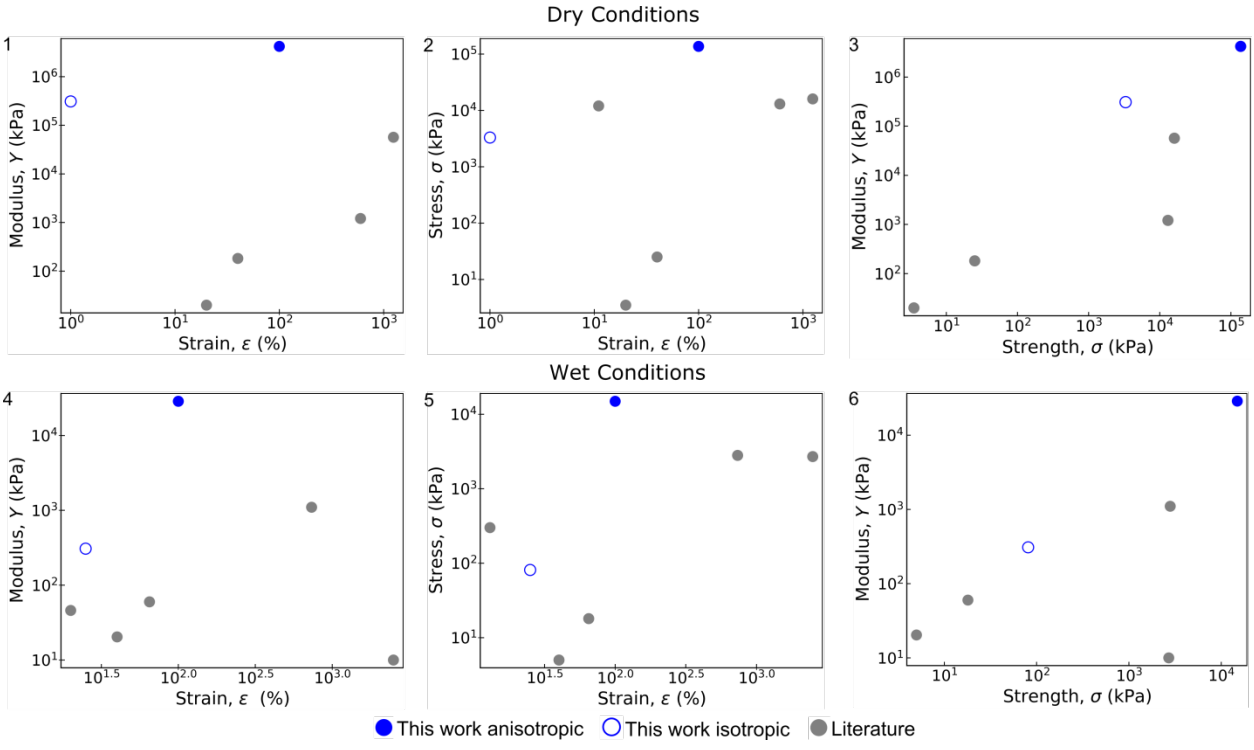

Supplementary Figure S10. Ashby plots comparing the mechanical properties of literature reported WTSM with the engineered SM keratin materials. Ashby plots correlating Young's modulus, tensile stress and max strain of the literature reported WTSM materials and the engineered keratin SM material both in dry and wet conditions. The graphs support the

importance of the anisotropic organization of the protofibrils in realizing the shape memory effect and allowing for the high mechanical performances of the material. Compared to the extruded material, the thin films are much more brittle and have lower tensile strength, both in dry and wet conditions. These films have mechanical properties more similar to literature reported WTSM materials.

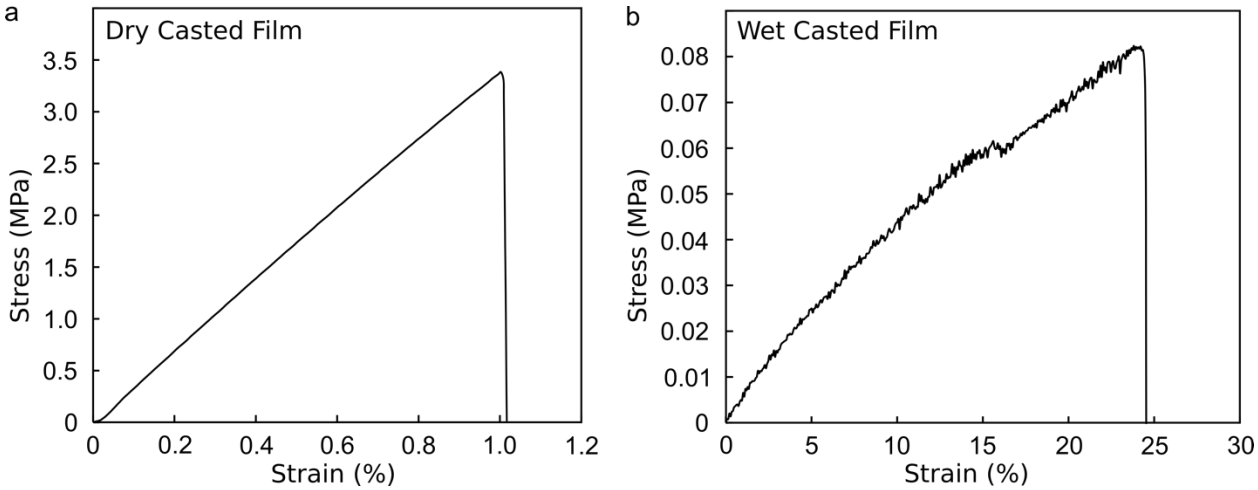

Supplementary Figure 11. Mechanical properties of isotropic casted keratin films. Representative stress-strain plots (representative of n = 3 curves) of cast keratin films (25×5×0.3 mm) in dry (left) and wet (right) conditions. Films were fabricated by casting the extracted keratin solution into acrylic moulds and inducing protein coagulation and cross-linking using a NaH_2PO_4 (0.8 M) and H_2O_2 (1% v/v) water bath. Compared to the extrusion process, the cast keratin material is much more brittle and has a lower tensile strength, both in dry (tensile strength of 3.29 ± 0.43 MPa and strain to failure of 1.02 ± 0.02 %) and wet (tensile strength of 81.5 ± 8.1 KPa and strain to failure of 25.3 ± 2.3 %) conditions. The decrease in mechanical performances due to the isotropic nanostructure of the casted film underscores the importance of protofibrils alignment to realize the shape memory effect. Data are presented as mean values, with experimental errors +/- calculated as SEM.

Chemical System	Trigger	Tensile Stress. kPa		Young's Modulus kPa		Max Strain (dry-wet)	Publication	Year
		Dry	Wet	Dry	Wet			
This Work (Anisotropic)	Water	>137,180	14,940	$4.2\times1E10^{+6}$	$28.7\times1E10^{+3}$	100-100%	/	/
This work (Isotropic)	Water	3,300	81	309000	308	1-25%		
Poly(butylene 2,5-furandicarboxylate)/Vinyl [10]	Water	25	5	182	20.36	40-40%	J. Mater. Chem. B	2019
tetra-poly(ethylene glycol)-based [11]	Water	13,000	2,700	1,210	10	600-2501%	Polym. Chem.	2019
*Silk-based [12]	Water	3.5	/	20	46	20%	Adv. Healthcare Mater.	2017
Gelatin [13]	Water	12000	300			11-13%	J. Mater. Chem. B	2017
Bovine Serum Albumin [14]	Water	/	18	/	60	65%	Nat. Commun	2019
Thermoplastic Polyurethatne [15]	Water	>16,000	2,800	56,800	1,100	1240-735%	RSC Adv.	2013

Supplementary Table 1. Mechanical properties of literature reported WTSM materials. Compared to the literature reported examples, both in dry and wet conditions, the tensile stress of our engineered material is one order of magnitude greater (dry = 137.18 ± 1.03 MPa, wet = 14.94 ± 0.46 MPa). The Young's modulus reaches even two orders of magnitude of difference, when in dry conditions (dry = 4.18 ± 0.10 GPa, wet = 28.7 ± 2.45). * The data are for compressive mechanical tests.

References

1 Paquin, R. & Colomban, P. *J. Raman Spectrosc*. **38**, 504-514 (2007).

2 Rodger A. *Far UV Protein Circular Dichroism*. *In: Roberts G.C.K. (eds) Encyclopedia of Biophysics*. (Springer, Berlin, Heidelberg 2013).

3 Smith, A. M., Banwell, E. F., Edwards, W. R., Pandya, M. J. & Woolfson D. N. Engineering Increased Stability into Self-Assembled Protein Fibers. *Adv. Funct. Mater*. **16**, 1022-1030 (2006).

4 Bernot, K. M., Lee, C.-H. & Coulombe, P. A. A small surface hydrophobic stripe in the coiled-coil domain of type I keratins mediates tetramer stability. *J. Cell Biol.* **168**, 965-974 (2005).

5 Sahajpal, V., Goyal, S., Singh, K. & Thakur, V. Dealing wildlife offences in India: role of the hair as physical evidence. *Int. J. Trichology* **1**, 18-26 (2009).

6 Li, Q., Brady, P. R. & Wang, X. Influence of pH on Hygral Expansion, Relaxation Shrinkage and Extensibility of Wool Fabric. *Fiber Polym*. **8**, 230-233 (2007).

7 Scott, D. L., Bradley, W. S. & Anderson, D. Kinetics and mechanism of the reaction of cysteine and hydrogen peroxide in aqueous solution. *J. Pharm. Sci.* **94**, 304-316 (2005).

8 Soomro, A., Alsop, R. J., Negishi, A., Kreplak, L., Fudge, D., R. Kuczmarski, E., Goldman, R. D. & Rheinstädter, M. C. *J. R. Soc. Interface* **14**, 20170123 (2017).

9 Busson, B., Briki, F. & Doucet, J. Side-Chains Configurations in Coiled Coils Revealed by the 5.15-Å Meridional Reflection on Hard a-Keratin X-Ray Diffraction Patterns. *J. Struct. Biol.* **125**, 1-10 (1999).

10 Guo, Y., Lv, Z., Huo, Y., Sun, L., Chen, S., Liu, Z., He, C., Xiaoping, Bi., Fanc, X. & You, Z. A biodegradable functional water-responsive shape memory polymer for biomedical applications. *J. Mater. Chem. B*, **7**, 123-132 (2019).

11 Tian, T., Wang, J., Wu, S., Shao, Z., Xiang, T. & Zhou, T. A body temperature and water-induced shape memory hydrogel with excellent mechanical properties. *Polym. Chem*. **10**, 3488-3496 (2019).

12 Brown, J. E., Moreau, J. E., Berman, A. M., McSherry, H. J., Coburn, J. M., Schmidt, D. F. & Kaplan, D. L. Shape Memory Silk Protein Sponges for Minimally Invasive Tissue Regeneration. *Adv. Healthcare Mater*. **6**, 1600762, (2017).

13 R. Zamani Alavijeh, R. Z., Shokrollahi, P. & Barzin J. A thermally and water activated shape memory gelatin physical hydrogel, with a gel point above the physiological temperature, for biomedical applications *J. Mater. Chem. B* **5**, 2302-2314 (2017).

14 Luai R. Khoury, L. R. & Popa, I. Chemical unfolding of protein domains induces shape change in programmed protein hydrogels. *Nat. Commun.* **10**, 5439 (2019).

15 Gu, x. & Mather P. T. Water-triggered shape memory of multiblock thermoplastic polyurethanes (TPUs). *RSC Adv*., **3**, 15783-15791 (2013).